RSC Advances

PAPER

View Article Online
View Journal | View Issue

Cite this: *RSC Adv.*, 2022, **12**, 30611

Inhibition performance of halogen-substituted benzaldehyde thiosemicarbazones as corrosion inhibitors for mild steel in hydrochloric acid solution†

Honghong Zhang, *[ab] Zhongnian Yang,[abc] Li Zhang,[a] Wu Yue,[a] Yanfeng Zhu[abc] and Xian Zhang[ac]

Received 9th September 2022
Accepted 19th October 2022

DOI: 10.1039/d2ra05690a

rsc.li/rsc-advances

Halogen-substituted benzaldehyde thiosemicarbazone derivatives were synthesized and their inhibition performance for mild steel in hydrochloric acid solution were investigated systematically using weight loss measurements, electrochemical techniques, scanning electron microscopy and quantum chemical calculations. Results of weight loss measurements indicated that all these compounds exhibited excellent inhibition performance and the inhibition efficiency increased with increasing inhibitor concentrations. Polarization results revealed that the synthesized benzaldehyde thiosemicarbazone derivatives were mixed-type inhibitors. Adsorption of these compounds onto a mild steel surface was mainly chemisorption and complied with the Langmuir adsorption isotherms. Both theoretical calculations and experimental measurements suggested that the inhibition efficiency of these compounds followed the order of Br-BT > Cl-BT > F-BT > H-BT.

1. Introduction

Corrosion of mild steel is inevitable and undesirable when applied in acid solutions.[1–3] Till now, great efforts have been made to reduce the corrosion rate of mild steel in acid environments.[4–6] Generally, the degradation of mild steel may be suppressed by surface engineering, organic coatings, electrical control (anodic and cathodic protection), and the application of passive alloys and corrosion inhibitors.[7–10] Deo[11] has electrodeposited single-phase Ni–Cu alloy coatings on mild steel surfaces. The corrosion potential for this coating moved positively in comparison with mild steel substrate and the corrosion rate was considerably reduced under the superior electrodeposition current density and deposition time. Wen[12] reported an intelligent alkyd coating containing BTA@PHVA/PEI nanocontainers on mild steel, which presented good thermal stability and high weight percentage of embedded inhibitors. Both electrochemical measurements and acid salt spray tests indicated excellent anti-corrosion ability of this intelligent coating. Bouoidina[13] investigated the protection property of three anisole derivatives for mild steel in 1 M HCl acid medium. Electrochemical studies suggested that these compounds were all good inhibitors with inhibition efficiency over 80%. Chafiq[14] found that hydrazone derivatives had a good inhibitory effect for mild steel in HCl solution and acted as mixed type inhibitors. The inhibition efficiency reaches 95% at the concentration of 5 mM. The excellent inhibition performance was further proved by the theoretical calculations. Loto[15] systematically studied the protection performance of zinc sacrificial anode on the cathodic protection of mild steel in HCl solution. Results indicated that the sacrificial anode can be efficiently applied both at low and high temperatures. Among all the above mentioned preventive methods, the addition of inhibitors has been considered to be one of the most popular and efficient methods for prevention of mild steel from corrosion in aggressive acid medium.[16–18]

Organic compounds in which molecular structure containing heteroatoms constitute of N, O, P and S and functional electronegative groups are thought to be excellent corrosion inhibitors, because they can be chemisorbed onto mild steel surface to form compact protective film and cover the active sites, thereby reduce the corrosion rate.[19–22] Berrissoul[23] studied the inhibition behavior of origanum compactum extract for mild steel in HCl solution. The findings revealed a high inhibition efficiency of 90% at 400 mg L^{-1} concentration. The presence of aromatic rings in the origanum compactum extract facilitated the adsorption behavior and consequently decreased

[a]Department of Chemical Engineering and Safety, Binzhou University, Binzhou, Shandong 256600, PR China. E-mail: bzuzhanghong@163.com; Tel: +86-18766499800

[b]Binzhou Key Laboratory of Aviation General Materials, Binzhou, Shandong 256600, PR China

[c]Binzhou Key Laboratory of Applied Electrochemistry, Binzhou, Shandong 256600, PR China

† Electronic supplementary information (ESI) available. See DOI: https://doi.org/10.1039/d2ra05690a

the metal degradation process. Poly[3-butyl-1-vinylimidazolium bromide] has been synthesized and served as a good corrosion inhibitor for mild steel in hydrochloric solution.[24] Polarization results indicated that this polymeric ionic liquid was a mixed type inhibitor and the inhibition efficiency exceeded 96%. The nitrogen atoms in this inhibitor molecules played an important role in the adsorption of poly[3-butyl-1-vinylimidazolium bromide] on mild steel surface. El Aoufir[25] prepared two triazole derivatives and investigated their inhibition property for mild steel in HCl solution. The triazole derivative with a longer carbon chain showed higher inhibition efficiency of 92% at concentration of 1 mM.

Based on the above considerations, thiosemicarbazone derivatives have been reported to be potential inhibitors for metal materials as their molecular structure contains N, O and S heteroatoms and aromatic rings.[26–28] Abd-El-Nabey[29] synthesized three benzaldehyde thiosemicarbazone derivatives for mild steel corrosion in 3.0 M H_3PO_4 solution. Electrochemical measurements suggested that these compounds acted as mixed-type inhibitors and the inhibition efficiencies were over 95% at proper concentrations. Zaidon[30] synthesized four benzaldehyde thiosemicarbazone derivatives and investigated their inhibition performance for mild steel in 1.0 HCl medium from both experimental and thermotical aspects. The obtained 2-(4-chlorobenzylidene)-*N*-phenylhydrazinecarbothioamide exhibited the greatest inhibition efficiency of 93.38%. Meanwhile, in our previous work,[31,32] different benzaldehyde thiosemicarbazone derivatives were synthesized and these compounds exhibited excellent corrosion protection performance. However, litter work appears to have been done on the inhibition behavior of mild steel in hydrochloric acid using different halogen-substituted benzaldehyde thiosemicarbazone derivatives. In the present work, halogen-substituted and non-halogen-substituted benzaldehyde thiosemicarbazone were prepared (Table 1). The aim of this study is to systematically investigate the effect of halogen element on the inhibition properties of benzaldehyde thiosemicarbazone derivatives for mild steel in hydrochloric solution using weight loss measurement, electrochemical tests and quantum chemical calculations.

2. Experimental

2.1 Materials

Fig. 1 shows the preparation scheme of the investigated benzaldehyde thiosemicarbazone derivatives that synthesized based on our previous work.[32] The molecular structure, abbreviations and structure characterizations of these synthesized benzaldehyde thiosemicarbazone derivatives are presented in Table 1. The obtained benzaldehyde thiosemicarbazone derivatives were purified and structurally characterized. The melting point of synthesized H-BT, F-BT, Cl-BT and Br-BT were found to be 163–166, 202–204, 207–211 and 214–217 °C, respectively. The FT-IR spectrum of these chemicals shows some main absorption band at 3380–3450 cm^{-1} (N–H), 1590–1610 cm^{-1} (C=N, C=C) and 860 cm^{-1} (C=S).

The aggressive electrolyte of 1.0 M HCl solution was prepared from the dilution of an analytical grade 37 wt% HCl with de-ionized water.

2.2 Weight loss experiments

Weight loss tests were performed by placing the mild steel samples (dimension 5 × 2.5 × 0.5 cm) in the 500 mL of 1.0 M HCl solution in the absence and presence of different concentrations of benzaldehyde thiosemicarbazone derivatives in a thermostat water bath. The samples were accurately weighted

Table 1 Molecular structures, abbreviations and structure characterizations of the synthesized benzaldehyde thiosemicarbazone derivatives

No.	Molecular structures	Abbreviations	Structure characterizations
1	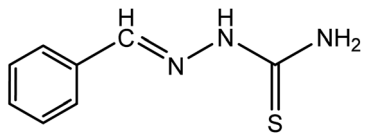	H-BT	$C_8H_9N_3S$ (mol. wt. 179), M.P. 163–166 °C, IR spectrum (KBr, cm^{-1}) 3405, 3148, 1593, 864
2	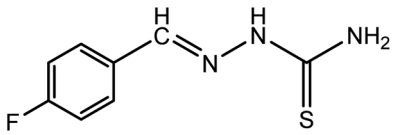	F-BT	$C_8H_8N_3SF$ (mol. wt. 197), M.P. 202–204 °C, IR spectrum (KBr, cm^{-1}), 3389, 3157, 1599, 862
3	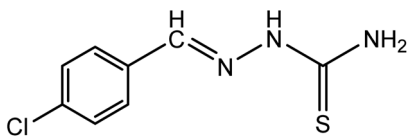	Cl-BT	$C_8H_8N_3SCl$ (mol. wt. 213.5), M.P. 207–211 °C, IR spectrum (KBr, cm^{-1}), 3431, 3166, 1601, 859
4	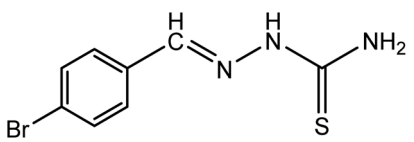	Br-BT	$C_8H_8N_3SBr$ (mol. wt. 257.9), M.P. 214–217 °C, IR spectrum (KBr, cm^{-1}), 3430, 3165, 1600, 861

Table 2 The weight loss results for mild steel in 1.0 M HCl solution without and with different concentrations of benzaldehyde thiosemicarbazone derivatives at 303 K with an immersion time of 8 h

Inhibitor	C_{inhi} (μM)	CR (mg cm^{-2} h^{-1})	η (%)	θ
Blank	0	6.85 ± 0.28	—	—
H-BT	50	3.08 ± 0.12	55.0	0.550
	100	2.01 ± 0.07	70.7	0.707
	200	1.24 ± 0.04	81.9	0.819
	300	0.87 ± 0.05	87.3	0.873
	400	0.59 ± 0.03	91.4	0.914
F-BT	50	2.80 ± 0.11	59.1	0.591
	100	1.66 ± 0.06	75.8	0.758
	200	1.14 ± 0.04	83.4	0.834
	300	0.65 ± 0.03	90.5	0.905
	400	0.51 ± 0.03	92.6	0.926
Cl-BT	50	2.67 ± 0.09	61.0	0.610
	100	1.42 ± 0.06	79.3	0.793
	200	0.96 ± 0.04	86.0	0.860
	300	0.56 ± 0.03	91.8	0.918
	400	0.40 ± 0.02	94.2	0.942
Br-BT	50	2.47 ± 0.11	63.9	0.639
	100	1.34 ± 0.04	80.4	0.804
	200	0.78 ± 0.03	88.6	0.886
	300	0.48 ± 0.02	93.0	0.930
	400	0.32 ± 0.01	95.3	0.953

before and after immersion of 8 h at various temperatures. Each condition was replicated three times to calculate the average value.

The corrosion rate (mg cm^{-2} h^{-1}) was calculated *via* the following equation:[33]

$$CR = \frac{87.6 \times W}{A \times t \times \rho} \quad (1)$$

where W is the mass loss (mg), A is the exposed area of 32.5 cm^2, t is immersion time of 8 h and ρ is the mild steel density of 7.86 × 10^3 g cm^{-3}.

2.3 Electrochemical measurements

Electrochemical experiments were conducted using CHI 660E electrochemical workstation with a standard three electrode system. A large platinum mesh and a saturated calomel electrode (SCE) were used as a counter and reference electrode, respectively. The mild steel retained an exposed surface of 0.50 cm^2, and the rest was encapsulated with Teflon. The working surface was initially polished with SiC abrasive paper, then cleaned using ethanol and de-ionized water before electrochemical tests. Electrochemical measurements were performed in 1.0 M HCl solution at 303 K without and with different concentrations of benzaldehyde thiosemicarbazone derivatives. For all electrochemical measurements, the working electrode should be immersed in the corrosive electrolyte for 1 h to obtain a stable open circuit potential (OCP). Potentiodynamic polarization plots were measured in the potential range from −250 mV to 250 mV (*vs.* E_{ocp}) with a scan rate of 0.5 mV s^{-1}. EIS data were recorded at E_{ocp} in the frequency range from 10^5 to 10^{-2} Hz with a sinusoidal voltage amplitude of 5 mV. The EIS data were analyzed using ZSimpWin software.

2.4 Surface investigation

The surface morphologies of mild steel after immersion in 1.0 M HCl solution without and with 400 μM H-BT, F-BT, Cl-BT and Br-BT inhibitors for 8 h at 303 K were observed by SEM (Hitachi SU-8010) with an accelerating voltage of 30 kV at 2000× magnification. The chemical compositions of corroded mild steel surface in the absence and presence of benzaldehyde thiosemicarbazone derivatives were also detected using EDX detector model coupled with SEM.

2.5 Theoretical calculations

Quantum chemical calculations were conducted using density functional theory (DFT) with B3LYP/6-31G(d, p) according to our previous study.[32] Some useful quantum chemical parameters, such as the energy of the highest occupied molecular (E_{HOMO}), energy of the lowest unoccupied molecular orbital (E_{LUMO}), dipole moment (μ) and electronegativity (χ) were calculated to further analyze the correlation between the inhibitor molecular structure and inhibition performance.

3. Results and discussion

3.1 Weight loss measurements

Table 2 shows the results of weight loss measurements for mild steel in 1.0 M HCl solution without and with different concentrations of benzaldehyde thiosemicarbazone derivatives at 303 K. The inhibition efficiency (η%) and surface coverage (θ) were obtained from the following equation:[34]

$$\eta\ (\%) = (1 - CR_{inhi}/CR_{free}) \times 100 \quad (2)$$

$$\theta = 1 - CR_{inhi}/CR_{free} \quad (3)$$

where CR_{free} and CR_{inhi} correspond to the obtained corrosion rate for mild steel in 1.0 M HCl solution without and with various concentrations of benzaldehyde thiosemicarbazone derivatives, respectively. It is apparent that adding these benzaldehyde thiosemicarbazone derivatives effectively suppresses the corrosion rate of mild steel in hydrochloric acid solution. With increasing the inhibitor concentrations, the corrosion rate becomes smaller and the inhibition efficiency gets larger, suggesting the formation of stronger adsorption layer onto mild steel surface at higher inhibitor concentrations for both the halogen-substituted and non-halogen-substituted benzaldehyde thiosemicarbazone molecules. Meanwhile, the inhibition efficiency of halogen-substituted benzaldehyde thiosemicarbazone always presents larger values than that of the

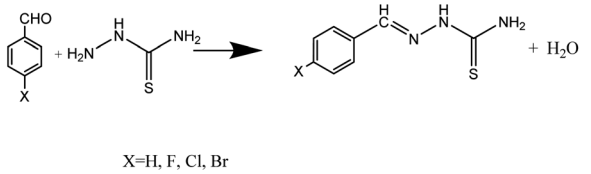

Fig. 1 Preparation scheme of studied benzaldehyde thiosemicarbazone derivatives.

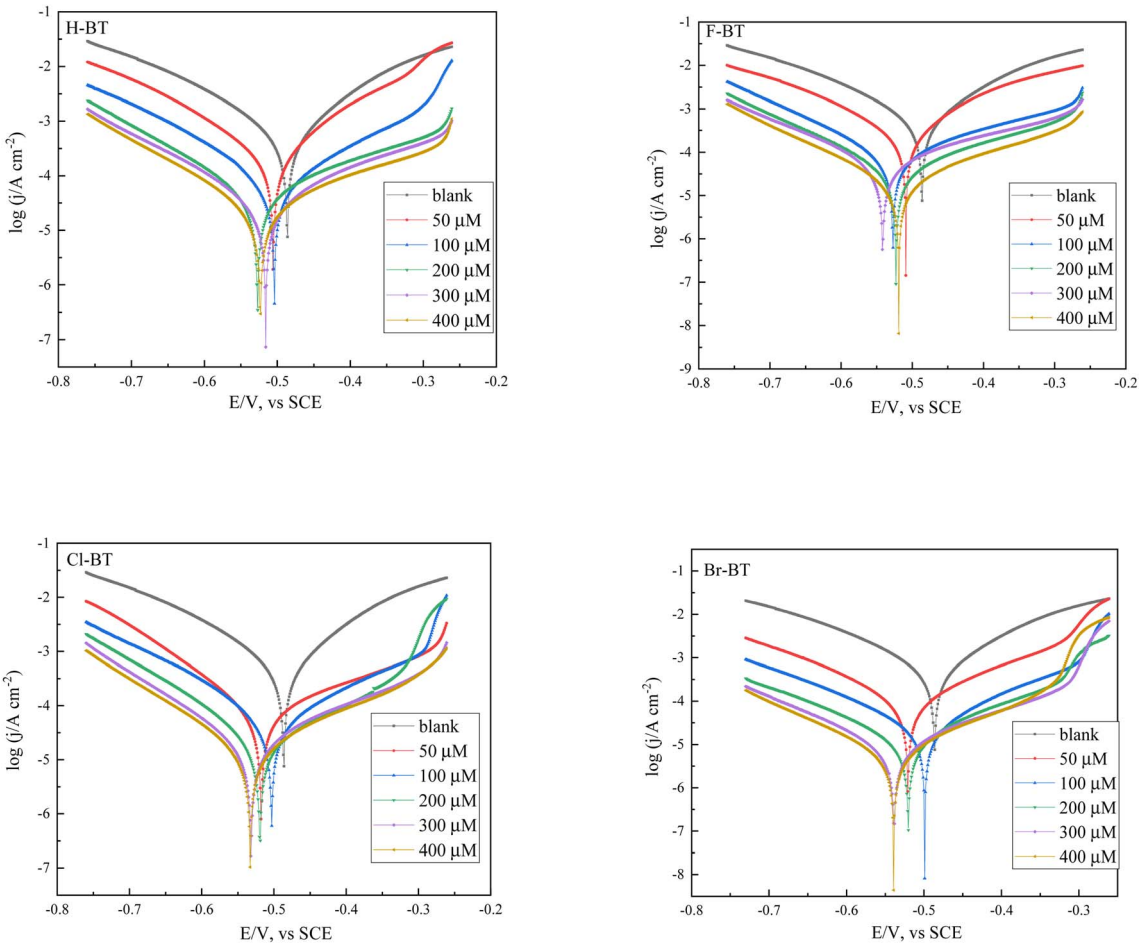

Fig. 2 Potentiodynamic polarization plots for mild steel in 1.0 M HCl solution without and with different concentrations of benzaldehyde thiosemicarbazone derivatives at 303 K.

non-halogen-substituted benzaldehyde thiosemicarbazone at the same concentration, revealing the positive effect of halogen element in the molecular structure on the inhibition performance. This phenomenon has also been reported previously.[35,36] The inhibition efficiency was found to follow the order: Br-BT > Cl-BT > F-BT > H-BT, and reaches the maximum value of 95.3%, 94.2%, 92.6% and 91.4%, respectively at the concentration of 400 μM, suggesting that the synthesized halogen-substituted and non-halogen-substituted benzaldehyde thiosemicarbazone acts as efficient corrosion inhibitors for mild steel in hydrochloric acid solution. Besides, Br atoms play a more important role in anti-corrosion performance compared with Cl and F atoms.

3.2 Potentiodynamic polarization curves

Potentiodynamic polarization plots for mild steel in 1.0 M HCl solution without and with different concentrations of benzaldehyde thiosemicarbazone derivatives at 303 K are presented in Fig. 2. The addition of these benzaldehyde thiosemicarbazone derivatives causes an obvious movement of both the anodic and cathodic Tafel branches toward lower current densities. This phenomenon suggests that both the anodic dissolution reaction and cathodic hydrogen evolution process are inhibited due to the adsorption of benzaldehyde thiosemicarbazone derivatives on the mild steel surface.[37] It also can be seen that the current density shows smaller values at larger inhibitor concentrations. Electrochemical parameters such as corrosion potential (E_{corr}), Tafel slopes (β_a and β_c) and corrosion current density (i_{corr}) were calculated by Tafel extrapolation method and provided in Table 3. The inhibition efficiency (η_T%) was obtained *via* eqn (4) and also presented.[38,39]

$$\eta_T\% = (1 - i_{corr}^{inhi}/i_{corr}^{0}) \times 100\% \quad (4)$$

where i_{corr}^{0} and i_{corr}^{inhi} represent the corrosion current densities for the corrosion of mild steel in 1.0 M hydrochloric acid solution without and with different concentrations of benzaldehyde thiosemicarbazone derivatives, respectively.

In the presence of benzaldehyde thiosemicarbazone derivatives, the corrosion potential moves negatively, but the shifts are all less than 55 mV (*vs.* SCE) in comparison with that of the blank sample, demonstrating that the synthesized benzaldehyde thiosemicarbazone derivatives acted as mixed-type inhibitors. Inspection of Fig. 2 and Table 3, the shape of cathodic Tafel branch in the presence of benzaldehyde

Table 3 Electrochemical parameters obtained from potentiodynamic polarization tests for mild steel in 1.0 M HCl solution without and with different concentrations of benzaldehyde thiosemicarbazone derivatives at 303 K

Inhibitor	C_{inh} (μmol L^{-1})	E_{corr} (mV)	β_a (mV dec^{-1})	$-\beta_c$ (mV dec^{-1})	i_{corr} (μA cm^{-2})	η_T (%)
Blank	0	−486 ± 6	125 ± 2.24	105 ± 1.89	501 ± 0.56	
H-BT	50	−509 ± 8	135 ± 1.57	114 ± 1.57	258 ± 0.27	48.5
	100	−514 ± 5	123 ± 1.31	137 ± 1.62	193 ± 0.13	61.5
	200	−535 ± 6	127 ± 2.63	154 ± 1.31	114 ± 0.17	77.2
	300	−523 ± 4	124 ± 1.80	139 ± 1.19	79.8 ± 0.2	84.1
	400	−530 ± 4	138 ± 1.92	147 ± 1.24	62.1 ± 0.12	87.6
F-BT	50	−506 ± 6	134 ± 2.35	115 ± 1.56	229 ± 0.33	54.3
	100	−516 ± 5	115 ± 1.82	128 ± 1.35	158 ± 0.15	68.5
	200	−524 ± 8	118 ± 1.59	151 ± 1.47	105 ± 0.21	79.0
	300	−539 ± 6	129 ± 1.47	137 ± 1.28	66.6 ± 0.17	86.7
	400	−521 ± 9	120 ± 1.26	161 ± 1.42	45.6 ± 0.13	90.9
Cl-BT	50	−513 ± 4	124 ± 2.04	131 ± 1.67	213 ± 0.26	57.5
	100	−504 ± 7	133 ± 1.73	128 ± 1.25	132 ± 0.14	73.7
	200	−515 ± 8	140 ± 1.67	147 ± 1.41	86.2 ± 0.16	82.8
	300	−529 ± 6	126 ± 1.26	134 ± 1.36	54.6 ± 0.12	89.1
	400	−531 ± 8	121 ± 1.32	145 ± 1.32	42.0 ± 0.10	91.6
Br-BT	50	−513 ± 5	129 ± 2.13	119 ± 1.54	197 ± 0.34	60.7
	100	−498 ± 8	122 ± 1.62	144 ± 1.29	118 ± 0.18	76.4
	200	−512 ± 6	126 ± 1.74	151 ± 1.62	74.1 ± 0.12	85.2
	300	−541 ± 5	130 ± 1.41	157 ± 1.24	44.6 ± 0.14	91.1
	400	−539 ± 8	132 ± 1.27	145 ± 1.31	31.1 ± 0.11	93.8

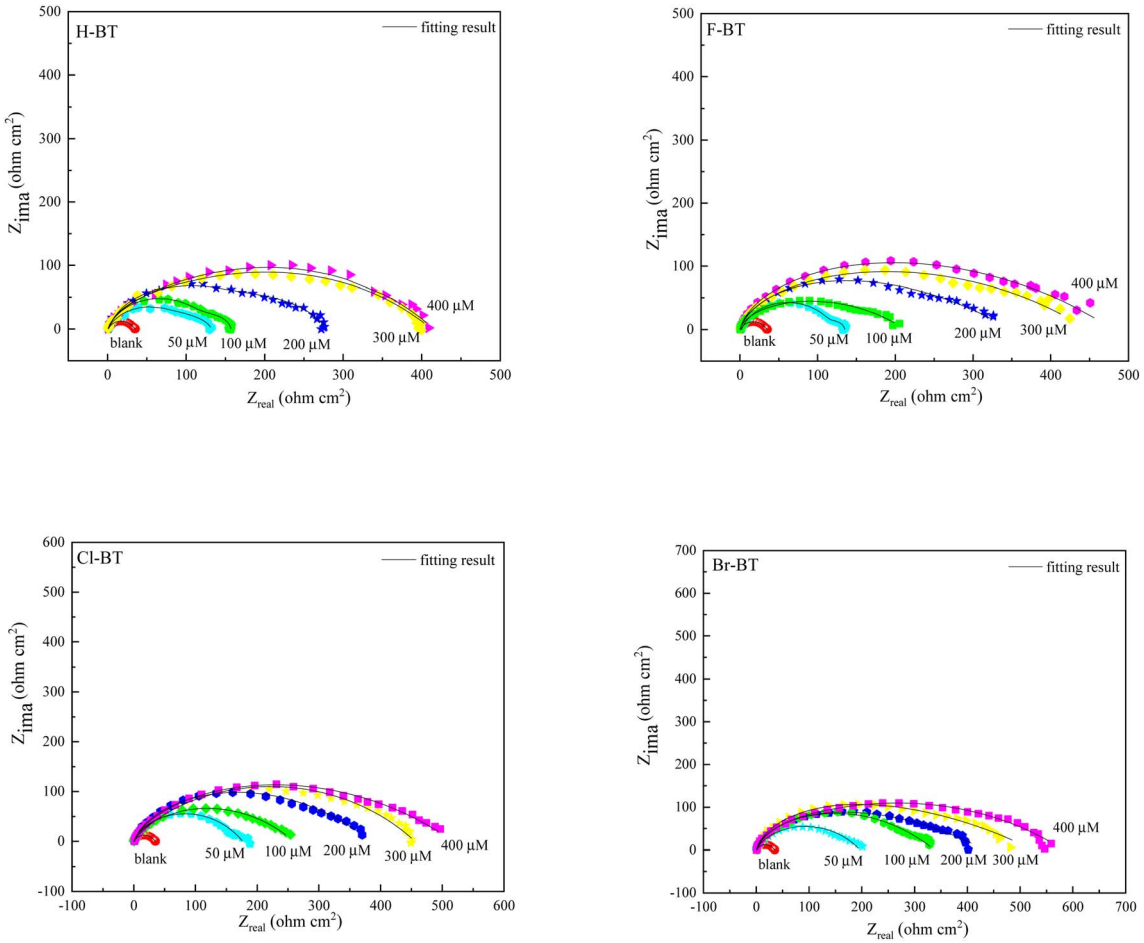

Fig. 3 Nyquist diagrams of mild steel in 1.0 M HCl solution without and with different concentrations of benzaldehyde thiosemicarbazone derivatives at 303 K.

thiosemicarbazone derivatives is almost the same to that of the blank case, meaning that the cathodic reaction is activation-controlled and the added benzaldehyde thiosemicarbazone derivatives did not change the hydrogen evolution mechanism.[40] The suppression of cathodic hydrogen evolution process was mainly ascribed to the fact the active sites of mild steel were covered by adsorbed benzaldehyde thiosemicarbazone derivatives molecules. However, the shape of anodic Tafel branch is much more pronounced affected, indicating that the anodic dissolution mechanism was considerably influenced by the adsorption of benzaldehyde thiosemicarbazone derivatives on mild steel surface to form Fe(II)-BT complex compound.[32] In addition, the corrosion current density was remarkably reduced with addition of benzaldehyde thiosemicarbazone derivatives and decreased gradually with increasing inhibitor concentrations. The fitted result also reveals that the inhibition efficiency complies with the order of Br-BT > Cl-BT > F-BT > H-BT, which is in good accordance with the gravimetric tests. The better inhibition performance of Br-substituted benzaldehyde thiosemicarbazone derivative in comparison with that of Cl and F may be due to the weaker induction effect of Br-substituted group.[35]

3.3 EIS measurements

Nyquist diagrams of mild steel in 1.0 M HCl solution without and with different concentrations of benzaldehyde thiosemicarbazone derivatives at 303 K are depicted in Fig. 3. The diameter of semicircles dramatically increases with addition of benzaldehyde thiosemicarbazone derivatives and continuously increases with enlarging inhibitor concentrations, revealing that the existence of benzaldehyde thiosemicarbazone derivatives can effectively hinder the degradation rate of mild steel in hydrochloric acid solution. As deduced through both the Nyquist diagrams (Fig. 3) and Bode plots features (Fig. S2†), the impedance spectra suggest one time constant for blank sample and two time constants in the presence of benzaldehyde thiosemicarbazone derivatives. The depressed semicircles in Nyquist plots reveal a non-ideal electrochemical behavior at the metal/electrolyte interface due to the surface roughness and inhomogeneity.[41] Thus, in the equivalent electrochemical circuit model, as shown in Fig. 4, a constant phase element CPE was employed to fit the EIS data. The impedance of CPE can be calculated *via* the following equation:[42,43]

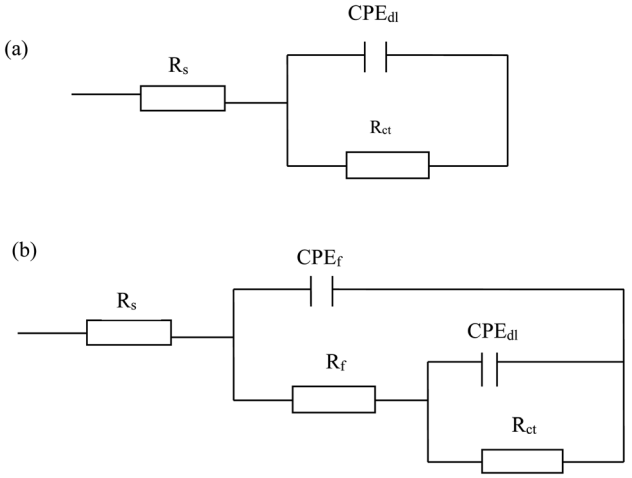

Fig. 4 Two models used for fitting the EIS data. R_s is solution resistance, CPE_{dl} and R_{ct} represent the double layer capacitance and charge transfer resistance, respectively. CPE_f and R_f correspond to the inhibitor film capacitance and film resistance, respectively.

$$Z_{CPE} = \frac{1}{Y_0(j\omega)^n} \quad (5)$$

Table 4 Electrochemical parameters obtained from EIS tests for mild steel in 1.0 M HCl solution without and with different concentrations of benzaldehyde thiosemicarbazone derivatives at 303 K

Inhibitor	C_{inh} (μM)	R_s (Ω cm^2)	R_f (Ω cm^2)	CPE_f (Ω^{-1} s^n cm^{-2})	n_f	R_{ct} (Ω cm^2)	CPE_{dl} (Ω^{-1} s^n cm^{-2})	n_{dl}	χ^2 10^{-3}	η_{EIS} (%)
Blank	0	1.17	—	—	—	32.1	193	0.92	0.86	—
H-BT	50	1.12	3.67	216	0.81	65.8	73.2	0.96	3.25	53.8
	100	1.24	7.82	193	0.83	125.4	38.6	0.95	2.64	75.9
	200	1.05	14.8	172	0.86	278.3	28.4	0.97	2.49	89.0
	300	1.07	21.3	135	0.85	386.4	21.7	0.98	2.72	92.1
	400	1.11	28.4	127	0.87	398.5	20.2	0.98	2.36	92.5
F-BT	50	0.99	8.39	208	0.82	122.6	47.2	0.95	0.73	75.5
	100	1.17	13.6	182	0.85	235.7	31.5	0.97	0.89	87.1
	200	1.06	19.8	157	0.84	342.2	22.8	0.98	0.92	91.1
	300	1.28	25.1	131	0.86	441.9	17.3	0.97	0.84	93.1
	400	1.21	34.3	119	0.87	472.3	16.6	0.98	0.80	93.7
Cl-BT	50	1.17	12.7	189	0.82	188.2	43.5	0.95	1.07	84.0
	100	1.12	18.1	178	0.84	265.3	30.2	0.97	0.82	88.7
	200	1.08	22.6	145	0.87	372.9	21.1	0.97	0.91	91.9
	300	1.16	28.9	127	0.86	467.5	15.4	0.98	1.53	93.5
	400	1.12	35.4	111	0.89	512.4	13.6	0.98	0.86	94.1
Br-BT	50	1.22	13.2	175	0.83	202.4	43.2	0.96	1.05	85.1
	100	1.28	20.5	157	0.85	267.9	31.4	0.97	0.93	88.9
	200	1.06	23.6	143	0.87	387.2	20.8	0.98	0.86	92.2
	300	1.15	31.3	124	0.87	478.8	15.3	0.98	0.92	93.7
	400	1.23	37.8	112	0.89	527.1	13.2	0.98	0.84	94.3

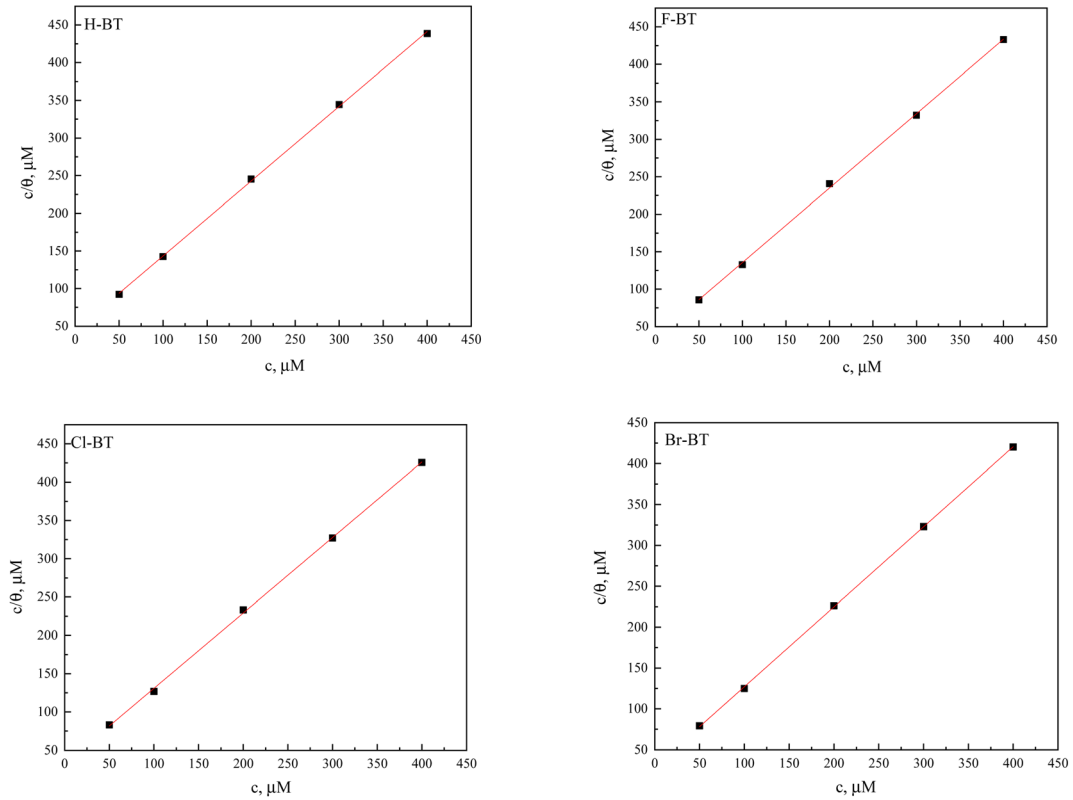

Fig. 5 Langmuir adsorption isotherm for benzaldehyde thiosemicarbazone derivatives on mild steel surface in 1.0 M HCl solution at 303 K.

Table 5 Thermodynamic parameters obtained from Langmuir adsorption isotherm

Inhibitor	K_{ads} ($\times 10^4$ M^{-1})	ΔG^0_{ads} (kJ mol^{-1})	Slope	R^2
H-BT	2.27	−35.4	0.993	0.999
F-BT	2.76	−35.9	0.993	0.999
Cl-BT	3.09	−36.2	0.985	0.999
Br-BT	3.43	−36.4	0.979	0.999

where ω is the angular frequency, and n is a deviation parameter that related to the surface inhomogeneity. The fitted electrochemical impedance parameters are summarized in Table 4. The polarization resistance R_P and inhibition efficiency η_{EIS} from EIS measurements are calculated as follows:[44]

Table 6 Gravimetric results of mild steel in 1.0 M HCl solution without and with 400 μM benzaldehyde thiosemicarbazone derivatives in the temperature range from 303 K to 333 K

Inhibitor	Temperature (K)	Blank CR (mg cm^{-2} h^{-1})	400 μM CR (mg cm^{-2} h^{-1})	η (%)
H-BT	303	6.85 ± 0.28	0.59 ± 0.03	91.4
	313	8.13 ± 0.25	0.64 ± 0.03	92.1
	323	9.71 ± 0.31	0.69 ± 0.02	92.9
	333	12.14 ± 0.35	0.74 ± 0.02	93.9
F-BT	303	6.85 ± 0.28	0.51 ± 0.03	92.6
	313	8.13 ± 0.25	0.57 ± 0.02	93.0
	323	9.71 ± 0.31	0.63 ± 0.03	93.5
	333	12.14 ± 0.35	0.69 ± 0.02	94.3
Cl-BT	303	6.85 ± 0.28	0.40 ± 0.02	94.2
	313	8.13 ± 0.25	0.42 ± 0.02	94.8
	323	9.71 ± 0.31	0.44 ± 0.01	95.5
	333	12.14 ± 0.35	0.47 ± 0.02	96.1
Br-BT	303	6.85 ± 0.28	0.32 ± 0.01	95.3
	313	8.13 ± 0.25	0.34 ± 0.02	95.8
	323	9.71 ± 0.31	0.37 ± 0.02	96.2
	333	12.14 ± 0.35	0.40 ± 0.01	96.7

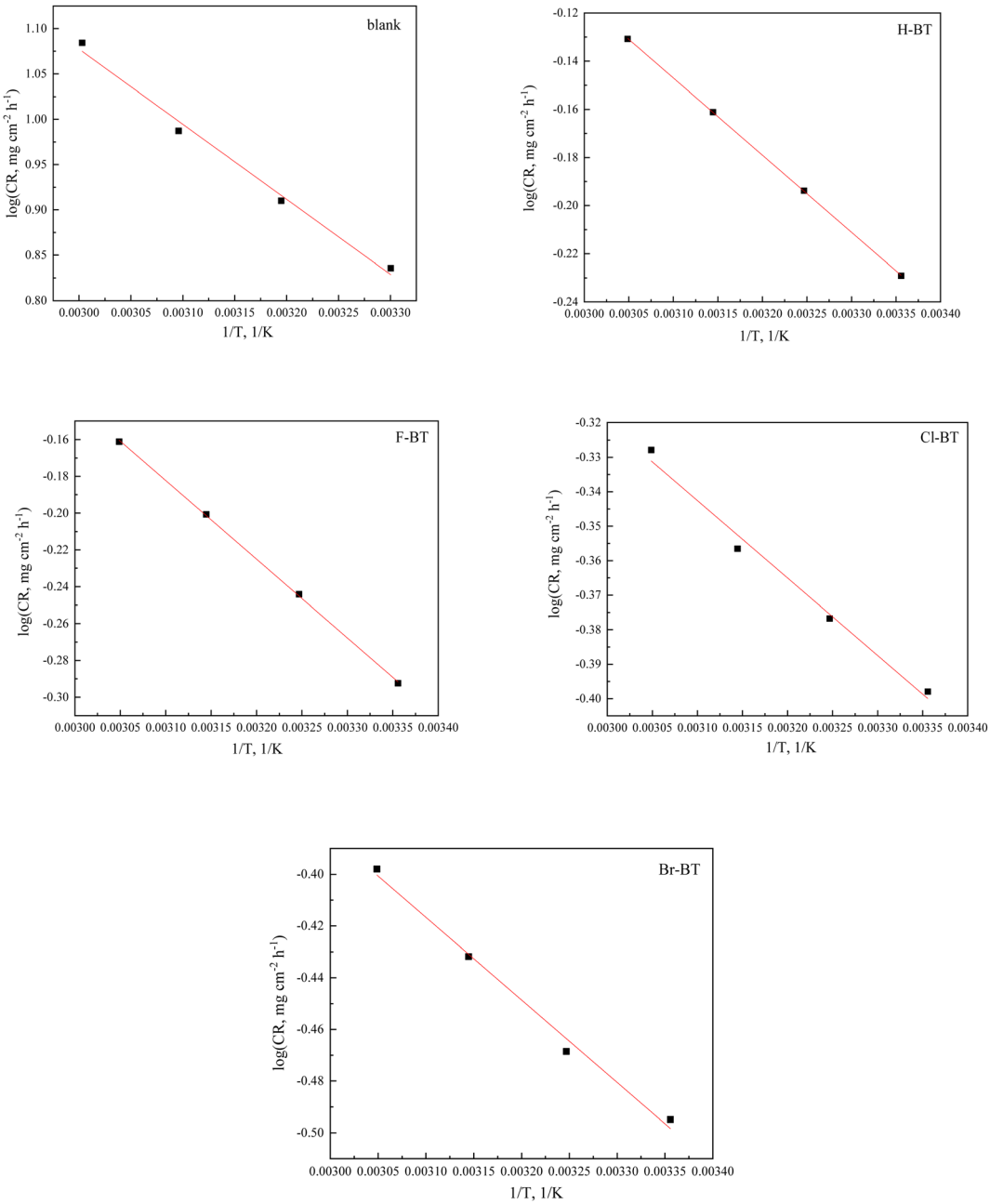

Fig. 6 Arrhenius plots of log CR *vs.* 1/*T* without and with 400 μM H-BT, F-BT, Cl-BT and Br-BT inhibitors.

$$R_P = R_{ct} + R_f \quad (6)$$

$$\eta_{EIS}\% = \frac{R_P^{inhi} - R_P^0}{R_P^{inhi}} \quad (7)$$

where R_P^0 and R_P^{inhi} are the polarization resistance in the absence and presence of different concentrations of benzaldehyde thiosemicarbazone derivatives, respectively. The results in Table 4 indicate that both R_f and R_{ct} values increase with increasing inhibitor concentrations and the values of CPE_{dl} show the opposite variation trend, suggesting the successful adsorption of benzaldehyde thiosemicarbazone derivatives on mild steel surface and the previously adsorbed water molecules were substituted by the inhibitor molecules. The value of n supplies information about the surface roughness of mild steel that a small value of n always reflects a relatively rough surface. It is worth noting that the value of n is larger in the presence of

Table 7 The apparent activation energy for mild steel in 1.0 M HCl solution without and with 400 μM H-BT, F-BT, Cl-BT and Br-BT inhibitors

Inhibitor	E_a (kJ mol^{-1})
Blank	14.2
H-BT	8.83
F-BT	8.57
Cl-BT	8.38
Br-BT	8.12

Table 8 Comparison of the inhibition efficiencies of different benzaldehyde thiosemicarbazone inhibitors for different temperatures

Inhibitor	Electrolyte	Temperature (K)	Inhibition efficiency (%)	Ref. No.
4-(*N*,*N*-Diethylamino)benzaldehyde thiosemicarbazone	0.67 M H_3PO_4	303	90.18	28
		308	88.75	
		313	86.71	
		318	85.69	
		323	80.49	
Benzaldehyde thiosemicarbazone	3 M H_3PO_4	303	97	29
para-Chlorobenzaldehyde thiosemicarbazone			96	
4-(Dimethylamino)benzaldehyde thiosemicarbazone			93	
2-Benzylidene-*N*-phenylhydrazine carbothioamide	1.0 M HCl	—	87.94	30
2-(4-Hydroxybenzylidene)-*N*-phenylhydrazinecarbothioamide			92.41	
2-(4-Chlorobenzylidene)-*N*-phenylhydrazinecarbothioamide			93.38	
2-(4-Methylbenzylidene)-*N*-phenylhydrazinecarbothioamide			90.08	
Benzaldehyde thiosemicarbazone	0.2 M Na_2SO_4	303	86.29	51
4-Methoxy benzaldehyde thiosemicarbazone			91.30	
4-Ethyl benzaldehyde thiosemicarbazone			95.39	
4-Bromo benzaldehyde thiosemicarbazone			90.04	
4-(*N*,*N*-Diethylamino)benzaldehyde thiosemicarbazone	1.0 M HCl	298	95.7	52
	1 M H_2SO_4	298	97.8	

benzaldehyde thiosemicarbazone derivatives than that of the blank, suggesting the less corroded surface of mild steel in hydrochloric acid solution. When the concentration was 400 μM, the inhibition efficiencies η_{EIS} for H-BT, F-BT, Cl-BT and Br-BT inhibitors were 92.5%, 93.7%, 94.1% and 94.3%, respectively. The halogen element in the molecular structure enhanced the inhibition performance as we analyzed from weight loss and polarization measurements. Meanwhile, the low values of the goodness of fit (χ^2) in Table 4 demonstrates that the fitted date agree well with the experimental data, indicating the validity of the proposed two equivalent circuit models.

3.4 Adsorption isotherm

Adsorption isotherm provides important information on the adsorption mechanism of organic inhibitors on mild steel surface. In the present work, the Langmuir adsorption isotherm[45,46] calculated *via* eqn (8) presents the best fitting result of weight loss measurements.

$$\frac{c}{\theta} = \frac{1}{K_{ads}} + c \tag{8}$$

Herein, θ is surface coverage which was obtained from weight loss tests in Table 2, K_{ads} is the equilibrium constant. According to eqn (8), the values of K_{ads} can be calculated by the intercept of Fig. 5. Then, the related thermodynamic parameter, the standard adsorption free energy ΔG^0_{ads} was derived from the following equation:[47]

$$K_{ads} = \frac{1}{55.5}\exp\left(\frac{-\Delta G^0_{ads}}{RT}\right) \tag{9}$$

where R and T are the ideal gas constant of 8.314 J mol^{-1} K^{-1} and thermodynamic temperature of 303 K, respectively. The values of K_{ads} and ΔG^0_{ads} are all listed in Table 5. The ΔG^0_{ads} of H-BT, F-BT, Cl-BT, Br-BT inhibitors were found to be −35.4, −35.9, −36.2 and −36.4 kJ mol^{-1}, respectively. The large negative ΔG^0_{ads} values reveal the spontaneous adsorption of benzaldehyde thiosemicarbazone derivatives on mild steel surface. Generally, the value of ΔG^0_{ads} lower than −40 kJ mol^{-1} indicates chemisorption that related to the charge transfer or sharing between the inhibitor molecules and metal atoms. Whereas the value of ΔG^0_{ads} larger than −20 kJ mol^{-1} suggests physisorption that owing to the electrostatic interaction between the inhibitor molecules and metal surface.[48] Therefore, the derived ΔG^0_{ads} values demonstrate that the benzaldehyde thiosemicarbazone derivatives adsorbed onto mild steel surface through both chemical and physical adsorption interaction. The heteroatoms of N, S and halogen, and aromatic rings in the molecular structure of benzaldehyde thiosemicarbazone derivatives which possess a number of lone pair of electrons, are considered to be active centers for adsorption process and facilitate the chemisorption on the mild steel surface. In addition, Br-BT inhibitor shows the largest value of K_{ads} and lowest value of ΔG^0_{ads}, suggesting the strongest adsorption capability on mild steel surface and presents the best anti corrosion performance.

3.5 Effect of temperature

Table 6 lists the gravimetric results of mild steel in 1.0 M HCl solution without and with 400 μM benzaldehyde thiosemicarbazone derivatives in the temperature range from 303 K to 333 K. As the testing temperature raised from 303 K to 333 K, the values of CR all increased, which was due to the accelerated dissolution of mild steel in hydrochloric acid solution at higher temperatures. It can be noticed that the dissolution rate of mild steel is slowed down mostly by the Br-BT inhibitor compared with other inhibitors. The apparent activation energy (E_a) can be calculated by the CR values according to the Arrhenius equation:[49,50]

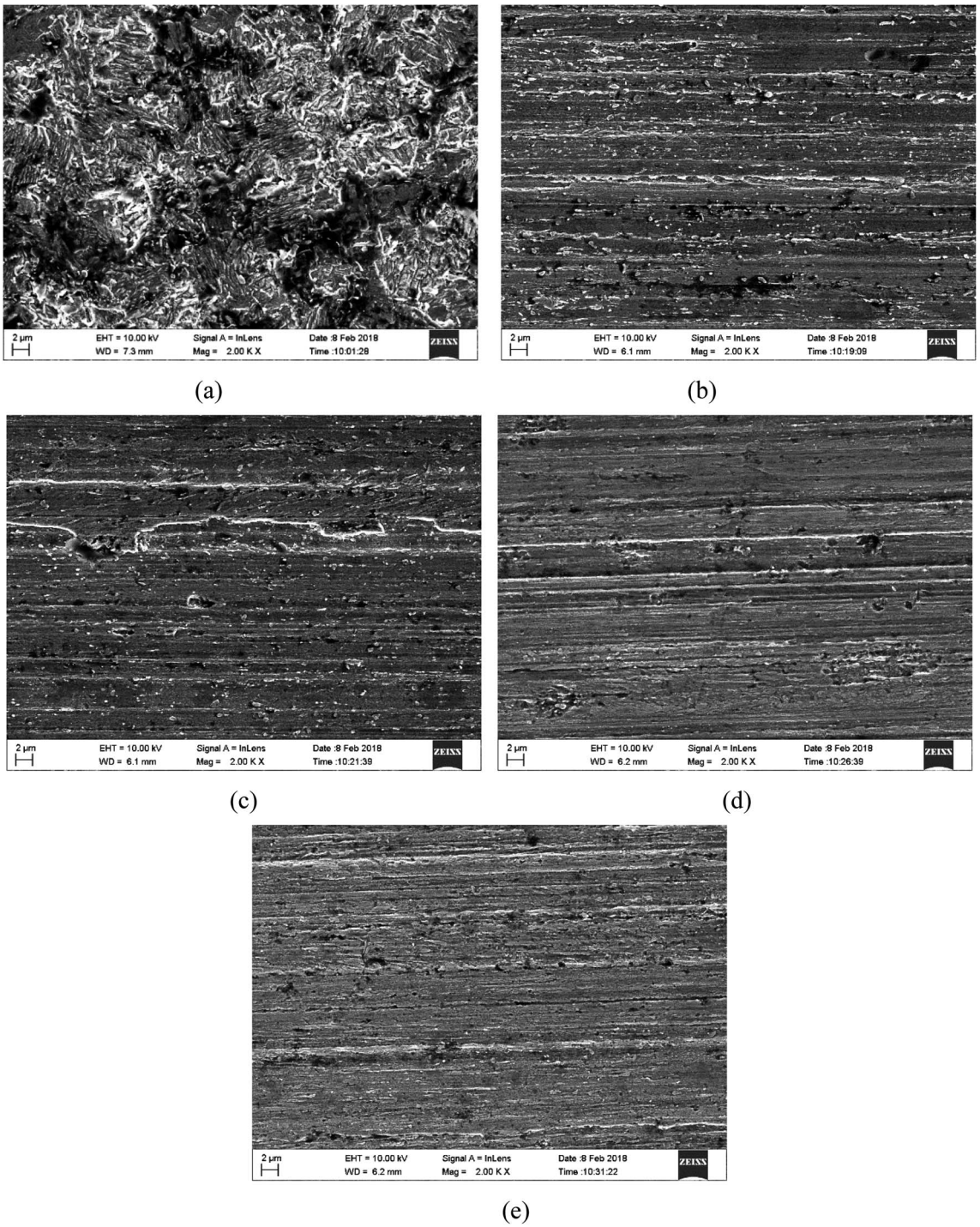

Fig. 7 SEM photos of mild steel surface immersed in 1.0 M HCl solution for 8 h at 303 K (a) without, with (b) 400 μM H-BT, (c) 400 μM F-BT, (d) 400 μM Cl-BT, (e) 400 μM Br-BT.

$$\log(\mathrm{CR}) = \frac{-E_a}{2.303RT} + \lambda \quad (10)$$

Herein, T is temperature, λ is the pre-exponential factor. The linear relationship can be observed from the straight lines of log(CR) *vs.* $1/T$ as shown in Fig. 6. The values of calculated E_a without and with 400 μM benzaldehyde thiosemicarbazone derivatives are summarized in Table 7 and are calculated to be 14.2, 8.83, 8.57, 8.38 and 8.12 kJ mol^{-1} for the blank case, H-BT, F-BT, Cl-BT and Br-BT inhibitor, respectively. The smaller values of E_a in the presence of benzaldehyde thiosemicarbazone derivatives with respect to the blank sample indicates that the synthesized benzaldehyde thiosemicarbazone derivatives mainly chemisorbed onto mild steel surface.[32] This result

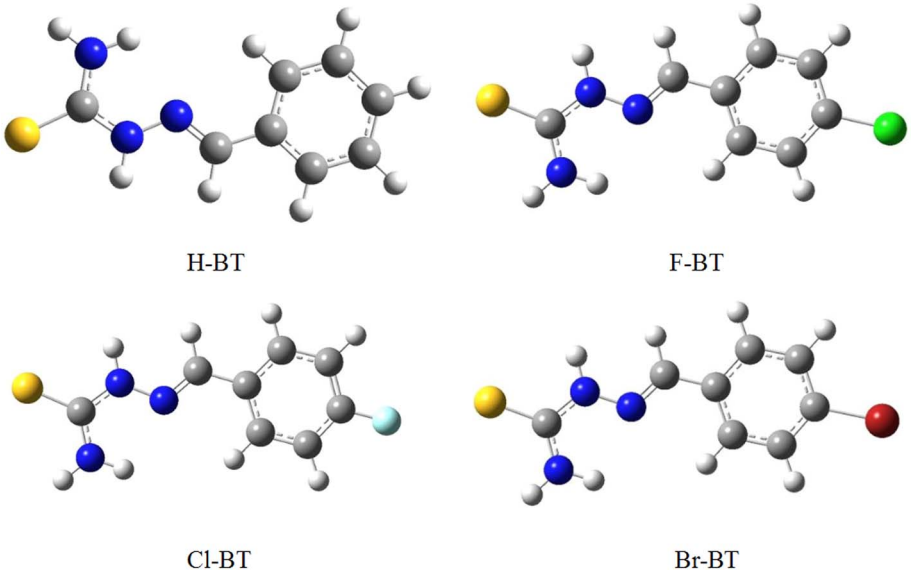

Fig. 8 Optimized structure of synthesized H-BT, F-BT, Cl-BT and Br-BT inhibitors.

matches well with Langmuir isotherm investigation. Table 8 lists the corrosion inhibition efficiencies of different benzaldehyde thiosemicarbazone derivatives at different testing temperatures. The synthesized halogen-substituted benzaldehyde thiosemicarbazone derivatives exhibited excellent corrosion protection property at high temperatures.

3.6 Surface investigation

The surface morphology of mild steel after immersion in 1.0 M HCl solution without and with 400 μM H-BT, F-BT, Cl-BT and Br-BT inhibitors for 8 h at 303 K are shown in Fig. 7. In the blank acid solution, the mild steel sample was severely damaged with obvious cavities and pits by the aggressive acid solution. However, with addition of 400 μM benzaldehyde thiosemicarbazone derivatives, the mild steel surface became smooth and the abrading scratches can be clearly observed, which was attributed to the protective performance of adsorbed benzaldehyde thiosemicarbazone derivatives molecules. It is noticeable that the mild steel surface with Br-BT inhibitor exhibited the least corroded cavities. The surface analysis implied that the synthesized benzaldehyde thiosemicarbazone derivatives are excellent corrosion inhibitors for mild steel in hydrochloric acid solution and Br-BT inhibitor presents the best anti corrosion behavior. EDX spectra were further performed to prove the successful adsorption of these benzaldehyde thiosemicarbazone derivatives molecules on mild steel surface, which results were shown in Fig. S3 and Table S1.† It is noticeable that no characteristic peaks for nitrogen (N) and sulfur (S) can be observed in the blank solution, while both of them were detected on Q235 mild steel surface in 1.0 M HCl solution containing 400 μM benzaldehyde thiosemicarbazone derivatives. The presence of these characteristic elements including halogen elements suggested the successful formation of a protective adsorption film of benzaldehyde thiosemicarbazone derivatives molecules on mild steel surface. Inspection of Table S1,† the percentage atomic content of Fe element was decreased in the presence of 400 μM benzaldehyde thiosemicarbazone derivatives in comparison with that of the absence, which was related to the surface coverage of these benzaldehyde thiosemicarbazone derivatives on mild steel surface.

3.7 Quantum chemical calculations

Quantum chemical calculations were performed to give deep insights into the correlation between the inhibitor molecular structure and inhibition property. Fig. 8 and 9 show the optimized structure and frontier molecule orbital density distributions of synthesized H-BT, F-BT, Cl-BT and Br-BT inhibitors, respectively. The classical quantum chemical parameters, such as E_{HOMO}, E_{LUMO}, energy gap ΔE ($E_{LUMO} - E_{HOMO}$), μ, χ, global hardness (ρ) and softness (σ) were calculated and summarized in Table 9. In general, the values of E_{HOMO} and E_{LUMO} are related to the electron donating ability and electron accepting capability, respectively, based on the frontier molecular orbital theory.[53] It is well accepted that the higher value of E_{HOMO} generally results in higher inhibition efficiency.[54] As seen from Table 9, the values of E_{HOMO} present the order of Br-BT > Cl-BT > F-BT > H-BT, indicating the best corrosion inhibition performance of Br-BT inhibitor, which is identical with our experimental measurements. According to the previous studies,[55,56] the smaller value of energy gap ΔE suggests a stronger chemical reactivity and thereby causes higher inhibition efficiency. The calculated ΔE values shows the variation trend of H-BT > F-BT > Cl-BT > Br-BT, revealing that the synthesized Br-BT inhibitor presents the strongest chemical reactivity and can be intensely adsorbed onto mild steel surface to form protective films.

The dipole moment μ also supplies some useful information to investigate the correlation between the inhibitor molecular

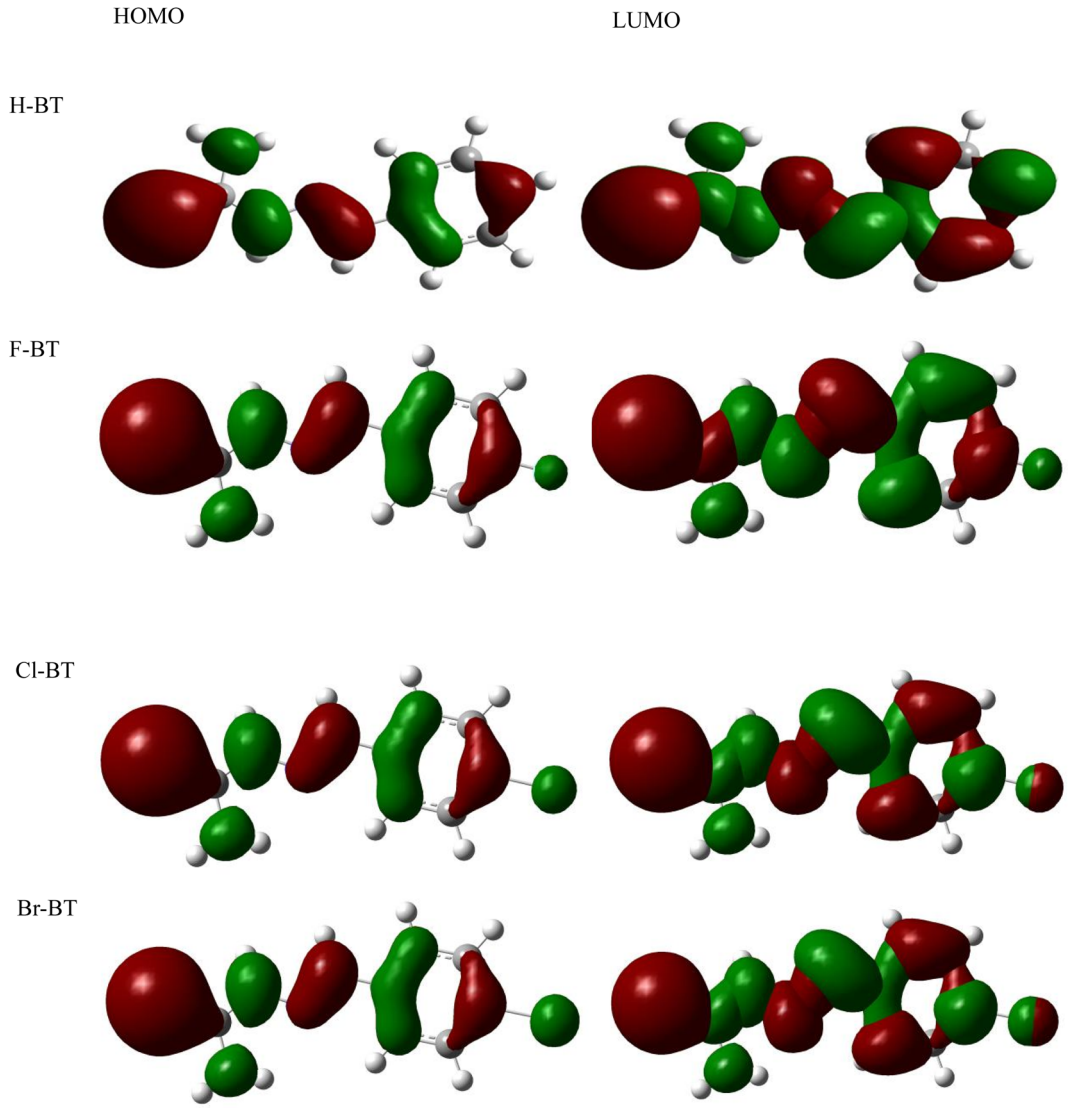

Fig. 9 Frontier molecule orbital density distributions of synthesized H-BT, F-BT, Cl-BT and Br-BT inhibitors.

structure and inhibition behavior. However, there still exists some controversy in the relationship between the dipole moment μ and inhibition efficiency. Some works suggested that a higher value of μ implies stronger adsorption of inhibitor molecules and thereby causes larger inhibition efficiency.[57,58] While some studies revealed the opposite conclusion that a higher value of μ represented smaller inhibition efficiency.[59,60] In this study, the dipole moment μ shows the order of H-BT > F-BT > Cl-BT > Br-BT, which is opposite to the inhibition efficiency from experimental tests. In addition, the electronegativity χ is another important parameter that is related to the freedom of electrons in the inhibitors. The Br-BT inhibitor possesses the largest value of electronegativity χ, revealing the best inhibition property.[61] The global hardness ρ also reflects the inhibition effect to some extent that a smaller value of ρ suggests a higher inhibition efficiency.[62] As shown in Table 9, the Br-BT inhibitor presents the smallest value of the global hardness ρ among all these inhibitors. The above results of E_{HOMO}, ΔE, μ and χ confirm the inference that Br atoms impact the charge distribution of benzaldehyde thiosemicarbazone derivatives and thus improve the inhibition effect. The interaction between adsorbed halogen-substituted benzaldehyde thiosemicarbazone derivatives and mild steel surface in the hydrochloric acid solution was through both electron-sharing and electrostatic interaction. The hydrated chloride ions are specifically adsorbed onto the electropositive mild steel surface to bring excess negative charges from the acid solution, enhancing the adsorption of cations. As a result of electrostatic interaction, the protonated benzaldehyde thiosemicarbazone derivatives are attracted toward the metal/electrolyte interface to form a protective film, preventing the metal from touching the acidic medium. Moreover, the benzaldehyde thiosemicarbazone derivatives may cover the mild steel surface by chemisorption mechanism at the same time, further retards the contact of mild steel surface with aggressive electrolyte. From the above

Table 9 Quantum chemical calculation results of synthesized H-BT, F-BT, Cl-BT and Br-BT inhibitors

Parameters	H-BT	F-BT	Cl-BT	Br-BT
E_{HOMO} (eV)	−5.9767	−6.0451	−6.0782	−6.0839
E_{LUMO} (eV)	−2.1467	−2.2243	−2.3364	−2.3565
ΔE (eV)	3.8300	3.8208	3.7418	3.7274
μ (D)	5.4560	3.7018	3.5031	3.5006
I (eV)	5.9767	6.0451	6.0782	6.0839
A (eV)	2.1467	2.2243	2.3364	2.3565
χ (eV)	4.0617	4.1346	4.2073	4.2202
ρ (eV)	−0.5734	−0.6121	−0.6682	−0.6783
σ $(eV)^{-1}$	−1.7441	−1.6336	−1.4966	−1.4744

analysis, the result of quantum chemical calculations confirms our experimental measurements.

4. Conclusions

Halogen-substituted benzaldehyde thiosemicarbazone derivatives were synthesized and their inhibition performance for mild steel in hydrochloric acid solution were investigated from both experimental and theoretical aspects. Results indicated that all these compounds are excellent corrosion inhibitors and the inhibition efficiency follows the order of Br-BT > Cl-BT > F-BT > H-BT. The inhibition efficiencies are over 90% for all these compounds at a concentration of 400 μM. Potentiodynamic polarization results suggested that the synthesized benzaldehyde thiosemicarbazone derivatives were mixed-type inhibitors and the inhibition efficiency increased with increasing inhibitor concentrations. Adsorption of these compounds onto mild steel surface was mainly chemisorption and conformed to the Langmuir adsorption isotherms. The results of quantum chemical calculations matched well with the experimental measurements.

Conflicts of interest

There are no conflicts to declare.

Acknowledgements

This work was supported by the Natural Science Foundation of Shandong Province (ZR2020ME018, ZR2021ME218, 2019KJC020, ZR2018LE002, ZR2022MB101) and the Major Project of Binzhou University (2019ZD02).

References

1 R. Aslam, M. Mobin, J. Aslam, H. Lagz, I.-M. Chung and S. Zehra, Synergistic inhibition behavior between rhodamine blue and cationic gemini surfactant on mild steel corrosion in 1 M HCl medium, *J. Mol. Struct.*, 2021, **1228**, 129751.

2 M. Faiz, A. Zahari, K. Awang and H. Hussin, Corrosion inhibition on mild steel in 1 M HCl solution by *Cryptocarya nigra* extracts and three of its constituents (alkaloids), *RSC Adv.*, 2020, **10**, 6547.

3 J. H. Tan, L. Guo, H. Yang, F. Zhang and Y. E. Bakri, Synergistic effect of potassium iodide and sodium dodecyl sulfonate on the corrosion inhibition of carbon steel in HCl medium: a combined experimental and theoretical investigation, *RSC Adv.*, 2020, **10**, 15163.

4 M. G. Mohamed, A. Mahdy, R. J. Obaid, M. A. Hegazy, S. W. Kuo and K. I. Aly, Synthesis and characterization of polybenzoxazine/clay hybrid nanocomposites for UV light shielding and anti-corrosion coatings on mild steel, *J. Polym. Res.*, 2021, **28**, 297–312.

5 S. R. Nayak, K. N. S. Mohana, M. B. Hegde, K. Rajitha, A. M. Madhusudhana and S. R. Naik, Functionalized multi-walled carbon nanotube/polyindole incorporated epoxy: an effective anti-corrosion coating material for mild steel, *J. Alloy. Compd.*, 2021, **856**, 158057.

6 M. M. Solomon, S. A. Umoren, M. A. Quraishi and M. Salman, Myristic acid based imidazoline derivative as effective corrosion inhibitor for steel in 15% HCl medium, *J. Colloid Interface Sci.*, 2019, **551**, 47–60.

7 R. K. Mehta, M. Yadav and I. B. Obot, Electrochemical and computational investigation of adsorption and corrosion inhibition behavior of 2-aminobenzohydrazide derivatives at mild steel surface in 15% HCl, *Mater. Chem. Phys.*, 2022, **290**, 126666.

8 E. Berdimurodov, A. Kholikov, K. Akbarov, G. B. Xu, A. M. Abdullah and M. Hosseimi, New anti-corrosion inhibitor (3ar, 6ar)-3a, 6a-di-*p*-tolyltetrahydroimidazo [4,5-*d*] imidazole-2,5(1*h*, 3*h*)-dithione for carbon steel in 1 M HCl medium: gravimetric, electrochemical, surface and quantum chemical analysis, *Arab. J. Chem.*, 2020, **13**, 7504–7523.

9 U. M. Angst, A critical review of the science and engineering of cathodic protection of steel in soil and concrete, *Corrosion*, 2019, **75**, 1420–1433.

10 M. J. Dai, J. Liu, F. Huang, Y. H. Zhang and Y. F. Cheng, Effect of cathodic protection potential fluctuations on pitting corrosion of X100 pipeline steel in acidic soil environment, *Corros. Sci.*, 2018, **142**, 428–437.

11 Y. Deo, S. Guha, K. Sarkar, P. Mohanta, D. Pradhan and A. Mondal, Electrodeposited Ni–Cu alloy coatings on mild steel for enhanced corrosion properties, *Appl. Surf. Sci.*, 2020, **515**, 146078.

12 J. X. Wen, J. L. Lei, J. L. Chen, J. J. Gou, Y. Li and L. J. Li, An intelligent coating based on pH-sensitive hybrid hydrogel for corrosion protection of mild steel, *Chem. Eng. J.*, 2020, **392**, 123742.

13 A. Bouoidina, E. Ech-chihbi, F. El-Hajjaji, B. El Ibrahimi, S. Kaya and M. Taleb, Anisole derivatives as sustainable-green inhibitors for mild steel corrosion in 1 M HCl: DFT and molecular dynamic simulations approach, *J. Mol. Liq.*, 2021, **324**, 115088.

14 M. Chafiq, A. Chaouiki, M. R. Al-Hadeethi, R. Salghi, H. A. Ismat, K. M. Shaaban and I.-M. Chung, A joint experimental and theoretical investigation of the corrosion inhibition behavior and mechanism of hydrazone

derivatives for mild steel in HCl solution, *Colloids Surf., A*, 2021, **610**, 125744.

15 C. A. Loto, R. T. Loto and A. P. Popoola, Performance evaluation of zinc anodes for cathodic protection of mild steel corrosion in HCl, *Chem. Data Collect.*, 2019, **24**, 100280.

16 M. Ouakki, M. Galai, Z. Benzekri, Z. Aribou, E. Ech-chihbi, L. Guo, K. Dahmani, K. Nouneh, S. Briche, S. Boukhris and M. Cherkaoui, *J. Mol. Liq.*, 2021, **334**, 117777.

17 M. J. Cui, S. M. Ren, H. C. Zhao, L. P. Wang and Q. J. Xue, Novel nitrogen doped carbon dots for corrosion inhibition of carbon steel in 1 M HCl solution, *Appl. Surf. Sci.*, 2018, **443**, 145–156.

18 F. E. Abeng, M. E. Ikpi, O. A. Ushie, V. C. Anadebe, B. E. Nyong, M. E. Obeten, N. A. Okafor, V. I. Chukwuike and P. Y. Nkom, Insight into corrosion inhibition mechanism of carbon steel in 2 M HCl electrolyte by eco-friendly based pharmaceutical drugs, *Chem. Data Collect.*, 2021, **34**, 100722.

19 M. Khattabi, F. Benhiba, S. Tabti, A. Djedouani, A. El Assyry, R. Touzani, I. Warad, H. Oudda and A. Zarrouk, Performance and computational studies of two soluble pyran derivatives as corrosion inhibitors for mild steel in HCl, *J. Mol. Struct.*, 2019, **1196**, 231–244.

20 H. Hassannejad and A. Nouri, Sunflower seed hull extract as a novel green corrosion inhibitor for mild steel in HCl solution, *J. Mol. Liq.*, 2018, **254**, 377–382.

21 P. Han, C. F. Chen, W. H. Li, H. B. Yu, Y. Z. Xu, L. Ma and Y. J. Zheng, Synergistic effect of mixing cationic and nonionic surfactants on corrosion inhibition of mild steel in HCl: experimental and theoretical investigations, *J. Colloid Interface Sci.*, 2018, **516**, 398–406.

22 W. W. Zhang, H. J. Li, L. W. Chen, S. Y. Zhang, Y. J. Ma, C. Ye, Y. Q. Zhou, B. Y. Pang and Y. C. Wu, Fructan from polygonatum cyrtonema hua as an eco-friendly corrosion inhibitor for mild steel in HCl media, *Carbohydr. Polym.*, 2020, **238**, 116216.

23 A. Berrissoul, A. Ouarhach, F. Benhiba, A. Romane, A. Guenbour, B. Dikici, F. Bentiss, A. Zarrouk and A. Dafali, Assessment of corrosion inhibition performance of origanum compactum extract for mild steel in 1 M HCl: weight loss, electrochemical, SEM/EDX, XPS, DFT and molecular dynamic simulation, *Ind. Crop. Prod.*, 2022, **187**, 115310.

24 E. K. Ardakani, E. Kowsari and A. Ehsani, Imidazolium-derived polymeric ionic liquid as a green inhibitor for corrosion inhibition of mild steel in 1.0 M HCl: experimental and computational study, *Colloids Surf., A*, 2020, **586**, 124195.

25 Y. El Aoufir, R. Aslam, F. Lazrak, R. Marzouki, S. Kaya, S. Skal, A. Ghanimi, I. H. Ali, A. Guenbour, H. Lgaz and I. M. Chung, The effect of the alkyl chain length on corrosion inhibition performances of 1,2,4-triazole-based compounds for mild steel in 1.0 M HCl: insights from experimental and theoretical studies, *J. Mol. Liq.*, 2020, **303**, 112631.

26 G. M. Pinto, J. Nayak and A. N. Shetty, Corrosion inhibition of 6061 Al-15 vol. pct. SiC(p) composite and its base alloy in a mixture of sulphuric acid and hydrochloric acid by 4-(*N*,*N*-diethylamino) benzaldehyde thiosemicarbazone, *Mater. Chem. Phys.*, 2011, **125**, 628–640.

27 E. Khamis, M. A. Ameer, N. M. Alandis and G. Al-Senani, Effect of thiosemicarbazones on corrosion of steel in phosphoric acid produced by wet process, *Corrosion*, 2000, **56**, 127–138.

28 T. Poornima, J. Nayak and A. N. Shetty, Effect of 4-(*N*,*N*-diethylamino)benzaldehyde thiosemicarbazone on the corrosion of aged 18 Ni 250 grade maraging steel in phosphoric acid solution, *Corros. Sci.*, 2011, **53**, 3688–3696.

29 B. A. Abd-El-Nabey, A. M. Abdel-Gaber, G. Y. Elewady, M. M. El Sadeek and H. Abd-El-Rhman, Inhibitive action of benzaldehyde thiosemicarbazones on the corrosion of mild steel in 3 M H_3PO_4, *Int. J. Electrochem. Sci.*, 2012, **7**, 11718–11733.

30 F. H. Zaidon, K. Kassim, H. M. Zaki, Z. Embong, E. H. Anouar and N. Z. N. Hashim, Adsorption and corrosion inhibition accomplishment for thiosemicarbazone derivatives for mild steel in 1.0 M HCl medium: electrochemical, XPS and DFT studies, *J. Mol. Liq.*, 2021, **329**, 115553.

31 H. H. Zhang, Y. Chen and Z. Zhang, Comparative studies of two benzaldehyde thiosemicarbazone derivatives as corrosion inhibitors for mild steel in 1.0 M HCl, *Results Phys.*, 2018, **11**, 554–563.

32 H. H. Zhang and Y. Chen, Experimental and theoretical studies of benzaldehyde thiosemicarbazone derivatives as corrosion inhibitors for mild steel in acid media, *J. Mol. Struct.*, 2019, **1177**, 90–100.

33 A. Batah, A. Chaouiki, O. E. El Mouden, M. Belkhaouda, L. Bammou and R. Salghi, Almond waste extract as an efficient organic compound for corrosion inhibition of carbon steel (C38) in HCl solution, *Sustainable Chem. Pharm.*, 2022, **27**, 100677.

34 J. T. Zhang, M. J. Kong, J. T. Feng, C. X. Yin, D. P. Li, L. Fan, Q. B. Chen and H. L. Liu, Dimeric imidazolium ionic liquids connected by bypyridiyl as a corrosion inhibitor for N80 carbon steel in HCl, *J. Mol. Liq.*, 2021, **344**, 117962.

35 K. G. Zhang, B. Xu, W. Z. Yang, X. S. Yin, Y. Liu and Y. Z. Chen, Halogen-substituted imidazoline derivatives as corrosion inhibitors for mild steel in hydrochloric acid solution, *Corros. Sci.*, 2015, **90**, 284–295.

36 Y. Xu, S. Zhang, L. Guo, B. Tan, C. Liao, Y. Zhou and L. H. Madkour, Halogen-substituted pyrazolo-pyrimidine derivatives as corrosion inhibitors for copper in sulfuric acid solution, *Int. J. Corros. Scale Inhib.*, 2018, **7**, 236–249.

37 A. Ramachandran, P. Anitha and S. Gnanavel, Structural and electronic impacts on corrosion inhibition activity of novel heterocyclic carboxamide derivatives on mild steel in 1 M HCl environment: experimental and theoretical approaches, *J. Mol. Liq.*, 2022, **359**, 119218.

38 Z. P. Mathew, K. Rajan, C. Augustine, B. Joseph and S. John, Corrosion inhibition of mild steel using poly(2-ethyl-2-oxazoline) in 0.1 M HCl solution, *Heliyon*, 2020, **6**, e05560.

39 S. Y. Cao, D. Liu, H. Ding, J. H. Wang, H. Lu and J. Z. Gui, Corrosion inhibition effects of a novel ionic liquid with

and without potassium iodide for carbon steel in 0.5 M HCl solution: an experimental study and theoretical calculation, *J. Mol. Liq.*, 2019, **275**, 729–740.

40 Z. Bensouda, E. Elassiri, M. Galai, M. Sfaira, A. Farah and M. E. Touhami, Corrosion inhibition of mild steel in 1 M HCl solution by *Artemisia abrotanum* essential oil as an eco-friendly inhibitor, *J. Mater. Environ. Sci.*, 2018, **9**, 1851–1865.

41 Y. Chen, Y. W. Liu, Y. Xie, H. H. Zhang and Z. Zhang, Preparation and anti-corrosion performance of superhydrophobic silane/graphene oxide composite coating on copper, *Surf. Coat. Technol.*, 2021, **423**, 127622.

42 Y. Chen, Y. W. Liu, Y. Xie, H. H. Zhang, X. Q. Du and Z. Zhang, Preparation of hydrophobic silane/graphene oxide composite coating implanted with benzotriazole to improve the anti-corrosion performance of copper, *J. Alloy. Compd.*, 2022, **893**, 162305.

43 X. Q. Du, Y. W. Liu, D. C. Chen, Z. Zhang and Y. Chen, Co-electrodeposition of silane and graphene oxide on copper to enhance the corrosion protection performance, *Surf. Coat. Technol.*, 2022, **436**, 128279.

44 H. H. Zhang, Y. W. Liu, H. Bian, Y. Zhang, Z. N. Yang, Z. Zhang and Y. Chen, Electrodeposition of silane/reduced graphene oxide nanocomposite on AA2024-T3 alloy with enhanced corrosion protection, chemical and mechanical stability, *J. Alloy. Compd.*, 2022, **911**, 165058.

45 R. Hsissou, O. Dagdag, S. About, F. Benhiba, M. Berradi, M. E. Bouchti, A. Berisha, N. Hajjaji and A. Elharfi, Novel derivative epoxy resin TGETET as a corrosion inhibition of E24 carbon steel in 1.0 M HCl solution. Experimental and computational (DFT and MD simulations) methods, *J. Mol. Liq.*, 2019, **284**, 182–192.

46 M. Damej, S. Kaya, B. E. Ibrahimi, H. S. Lee, A. Molhi, G. Serdaroğlu, M. Benmessaoud, I. H. Ali, S. E. Hajjaji and H. Lgaz, The corrosion inhibition and adsorption behavior of mercaptobenzimidazole and bis-mercaptobenzimidazole on carbon steel in 1.0 M HCl: experimental and computational insights, *Surf. Interfaces*, 2021, **24**, 101095.

47 R. Hsissou, S. About, R. Seghiri, M. Rehioui, A. Berisha, H. Erramli, M. Assouag and A. Elharfi, Evaluation of corrosion inhibition performance of phosphorus polymer for carbon steel in 1 M HCl: computational studies (DFT, MC and MD simulations), *J. Mater. Res. Technol.*, 2020, **9**, 2691–2703.

48 G. Bahlakeh, A. Dehghani, B. Ramezanzadeh and M. Ramezanzadeh, Highly effective mild steel corrosion inhibition in 1 M HCl solution by novel green aqueous mustard seed extract: experimental, electronic-scale DFT and atomic-scale MC/MD explorations, *J. Mol. Liq.*, 2019, **293**, 111559.

49 E. X. Ricky, M. Mpelwa and X. G. Xu, The study of *m*-pentadecylphenol on the inhibition of mild steel corrosion in 1 M HCl solution, *J. Ind. Eng. Chem.*, 2021, **101**, 359–371.

50 O. A. Akinbulumo, O. J. Odejobi and E. L. Odekanle, Thermodynamics and adsorption study of the corrosion inhibition of mild steel by *Euphorbia heterophylla* L. extract in 1.5 M HCl, *Results Mater.*, 2020, **5**, 100074.

51 S. T. Arab and K. M. Emran, Structure effect of some thiosemicarbazone derivatives on the corrosion inhibition of $Fe_{78}B_{13}Si_9$ glassy alloy in Na_2SO_4 solution, *Mater. Lett.*, 2008, **62**, 1022–1032.

52 P. Mourya, S. Banerjee, R. B. Rastogi and M. M. Singh, The inhibition of mild steel corrosion in hydrochloric and sulfuric acid media using thiosemicarbazone derivative, *Ind. Eng. Chem. Res.*, 2013, **52**, 12733–12747.

53 G. Bahlakeh, B. Ramezanzadeh, A. Dehghani and M. Ramezanzadeh, Novel cost-effective and high-performance green inhibitor based on aqueous *Peganum harmala* seed extract for mild steel corrosion in HCl solution: detailed experimental and electronic/atomic level computational explorations, *J. Mol. Liq.*, 2019, **283**, 174–195.

54 W. W. Zhang, H. J. Li, M. R. Wang, L. J. Wang, A. H. Zhang and Y. C. Wu, Highly effective inhibition of mild steel corrosion in HCl solution by using pyrido[1,2-a] benzimidazoles, *New J. Chem.*, 2019, **43**, 413.

55 N. M. El Basiony, A. Elgendy, H. Nady, M. A. Migahed and E. G. Zaki, Adsorption characteristics and inhibition effect of two Schiff base compounds on corrosion of mild steel in 0.5 M HCl solution: experimental, DFT studies and Monte Carlo simulation, *RSC Adv.*, 2019, **9**, 10473.

56 Y. J. Qiang, L. Guo, H. Li and X. J. Lan, Fabrication of environmentally friendly losartan potassium film for corrosion inhibition of mild steel in HCl medium, *Chem. Eng. J.*, 2021, **406**, 126863.

57 T. Laabaissi, F. Benhiba, Z. Rouifi, M. Rbaa, H. Oudda, H. Zarrok, B. Lakhrissi, A. Guenbour, I. Warad and A. Zarrouk, Benzodiazepine derivatives as corrosion inhibitors of carbon steel in HCl media: electrochemical and theoretical studies, *Prot. Met. Phys. Chem.*, 2019, **55**, 986–1000.

58 R. Hsissou, F. Benhiba, O. Dagdag, M. E. Bouchti, K. Nouneh, M. Assouag, S. Briche, A. Zarrouk and A. Elharfi, Development and potential performance of prepolymer in corrosion inhibition for carbon steel in 1.0 M HCl: outlooks from experimental and computational investigations, *J. Colloid Interface Sci.*, 2020, **574**, 43–60.

59 L. Jiang, Y. J. Qiang, Z. L. Lei, J. N. Wang, Z. J. Qin and B. Xiang, Excellent corrosion inhibition performance of novel quinoline derivatives on mild steel in HCl media: experimental and computational investigations, *J. Mol. Liq.*, 2018, **255**, 53–63.

60 N. Khalil, Quantum chemical approach of corrosion inhibition, *Electrochim. Acta*, 2003, **48**, 2635–2640.

61 M. A. Mostafa, A. M. Ashmawy, M. A. M. Abdel Reheim, M. A. Bedair and A. M. Abuelela, Molecular structure aspects and molecular reactivity of some triazole derivatives for corrosion inhibition of aluminum in 1 M HCl solution, *J. Mol. Struct.*, 2021, **1236**, 130292.

62 L. Herrag, B. Hammouti, S. Elkadiri, A. Aouniti, C. Jama, H. Vezin and F. Bentiss, Adsorption properties and inhibition of mild steel corrosion in hydrochloric solution by some newly synthesized diamine derivatives: experimental and theoretical investigations, *Corros. Sci.*, 2010, **52**, 3042–3051.